

Hemispheric asymmetry in the fusiform gyrus distinguishes *Homo sapiens* from chimpanzees

Steven A. Chance · Eva K. Sawyer ·
Linda M. Clover · Bridget Wicinski ·
Patrick R. Hof · Timothy J. Crow

Received: 17 April 2012 / Accepted: 6 October 2012 / Published online: 30 October 2012
© Springer-Verlag Berlin Heidelberg 2012

Abstract While the neural basis for linguistic communication has been linked to brain structural asymmetries found only in humans (wider connective spacing is found between the minicolumns of neurons in the left hemisphere language areas), it is unknown if the opposite microanatomical asymmetry exists in the fusiform gyrus which typically supports a right hemisphere bias for face processing. Unlike language, face processing is an ability shared with chimpanzees and, as Darwin observed, the widespread use of facial expressions in animal communication suggests a biological basis. We tested the principle that minicolumn asymmetry follows typical functional dominance in humans, and tested its evolutionary continuity, by measuring minicolumn width, neuronal size and density in the mid-fusiform cortex in 14 humans and 14 chimpanzees. We found that microanatomical asymmetry distinguishes humans from chimpanzees although the direction of asymmetry is the same as in language areas—the right hemisphere contained narrower minicolumns and smaller pyramidal neurons, as in auditory language areas. Uniformly narrow minicolumns in chimpanzees and in the human right hemisphere are consistent with mechanistic predictions supporting the apparent bias towards holistic

face processing. Wider minicolumns and larger neurons in the human left hemisphere may be consistent with a language function such as word-form processing. Microanatomical asymmetry in the neocortex therefore provides a correlate of hemispheric specialisation.

Keywords Minicolumn · Fusiform gyrus · Cerebral asymmetry · Primate · Evolution

Introduction

Some authors have suggested that cerebral asymmetry is a defining feature of the human brain central to the evolution of human cognition (e.g., Corballis 1992; Crow 2000). Among the earliest observations of localised cognitive functions in humans, Paul Broca and Carl Wernicke identified areas in the left hemisphere associated with linguistic aphasia. The anatomical asymmetry of the brain was rediscovered by Geschwind and Levitsky (1968) in their study of the planum temporale (part of Wernicke's area). It has since been suggested by some (Annett 1985; McManus 1985) that these asymmetries are human-specific and offer a neural correlate of lateralised function, including language, in humans.

A challenge to this thesis has emerged from comparative neuroanatomy indicating the presence of asymmetries in other primate species. Some comparative data suggest that gross brain asymmetries (“petalia”) are present in modern great apes (Holloway and De LaCoste-Lareymondie 1982). Other regional measures using MRI have found asymmetries in chimpanzee brain areas corresponding to Broca's area (the inferior frontal gyrus) in the frontal lobe (Cantalupo and Hopkins 2001) and Wernicke's area (area Tpt) in the temporal lobe (Gannon et al. 1998). However, more

S. A. Chance (✉) · E. K. Sawyer · L. M. Clover
Neuroanatomy and Cognition Group, Department of Clinical
Neurology, University of Oxford, Neuropathology, Level 1,
West Wing, JR Hospital, Oxford OX3 9DU, UK
e-mail: steven.chance@clneuro.ox.ac.uk

B. Wicinski · P. R. Hof
Fishberg Department of Neuroscience and Friedman
Brain Institute, Mount Sinai School of Medicine,
One Gustave Levy Place, New York, NY 10029, USA

T. J. Crow
POWIC, Warneford Hospital, Oxford OX3 7JX, UK

recent cytoarchitecturally defined assessments have found that region size asymmetries are weaker (Spocter et al. 2010) or absent in chimpanzees (Schenker et al. 2010) indicating that species differences may not be reliably detected at the level of gross region size. By contrast, assessments of hemispheric asymmetry at the neuronal level have found consistent differences between humans and other primates (Chance and Crow 2007). Asymmetry in the spacing of minicolumnar units of neurons in the human planum temporale is absent in the brains of other primates (Buxhoeveden et al. 2001) and there are more large layer III pyramidal neurons (Hutsler 2003) with wider dendritic arbors (Seldon 1981a, b) filling the space in the left hemisphere compared to the right in humans. Both Broca's area and Wernicke's area in humans have more connective neuropil in the left hemisphere compared to the right (Amunts et al. 1999; Anderson et al. 1999). In contrast, chimpanzees lack neuropil asymmetry in the equivalent areas (Sherwood et al. 2007). Neuron density in the equivalent of Wernicke's area, Tpt, in chimpanzees is not asymmetrical (Spocter et al. 2010). In Broca's area homologue in chimpanzees, minicolumn organisation, neuron number, and neuron density are also symmetrical (Schenker et al. 2010).

Yet, these studies of language areas do not separate the general question of the correspondence of structural asymmetry and functional lateralisation, from the specific case of language, which is unique to humans, raising the issue of whether microstructural asymmetry in association cortex exclusively follows the direction of hemispheric dominance for language. Another highly evolved ability in primates, face processing, provides a test case—it is the opposite of language, being dominant in the right hemisphere in humans (Kanwisher et al. 1997), and also a function successfully performed by our closest primate relative, the chimpanzee (Parr et al. 2009).

In the present study we have focused on measurement of minicolumn organisation, which has been proposed as a fundamental organising principle of cortical structure and function (for review, see Mountcastle 1997) and cell size. Established early by the radial units that form the cortex, minicolumns form a basis for the developmental and evolutionary expansion of cortical surface (for review, see Rakic 1995) and their spacing has, for example, been found to correlate with cortical surface area of the asymmetrical planum temporale (Chance et al. 2008). Definitions of minicolumns vary, partly depending on whether attention is focused on cell bodies or dendritic bundles. Most studies have focused on the vertical strings of cell bodies and define the column as either a single string of neurons or as an entity extending from the midline of one string of neurons, through the cell-sparse interval, to the midline of the adjacent string (Peters 2010). The measure we report

here combines both the neuron dense core and the neuropil periphery (see “Materials and methods” below).

The columnar organisation of cell bodies, axons and dendrite bundles is hypothesised to form the basis of microcircuits in the cortex (Mountcastle 1997), although scepticism, partly due to methodological variability, suggests that it may be overly optimistic to assert the columnar concept as “a unifying principle for understanding cortical function” (Horton and Adams 2005). However, minicolumn organisation has been found to correlate with cognitive scores in macaque monkeys (Cruz et al. 2009; a relationship that was specific to the region of cortex associated with the function rather than a neighbouring region), and humans (Chance et al. 2011; a relationship with cognition that was specific to minicolumn measures and was not found for neuron density).

In the auditory domain, it has been hypothesised that wider minicolumn spacing facilitates fine temporal discrimination whereas narrow minicolumn spacing supports broad spectral processing (Zatorre and Belin 2001). This emphasises type of processing over hemispheric dominance. Speech perception is therefore lateralised to the left auditory region because it requires fine discrimination of many short auditory signals while, in untrained listeners, music perception is dominant in the right hemisphere (Ono et al. 2011), where the minicolumns are narrow. By analogy, in the visual domain it is possible that wider minicolumn spacing may be associated with detailed feature processing whereas narrow minicolumns may facilitate holistic, configural processing of the type usually associated with face processing. In such a scheme, face processing is similar to music processing. This ‘processing-type’ hypothesis presents an alternative to the ‘dominance’ theory of wider minicolumns and predicts the opposite asymmetry in the fusiform region.

The processing-type hypothesis has the advantage of acknowledging the active role of the ‘non-dominant’ hemisphere. Just as different aspects of a function, such as sound processing, lateralise differently, it is recognised increasingly that many tasks combine elements of both holistic and featural processing. In the fusiform gyrus, visual objects are processed by both hemispheres and featural aspects of faces are processed by the left fusiform cortex (Rossion et al. 2000). In addition, the left fusiform region is dominant for processing another class of objects: visual word forms. Therefore, faces and words lateralise differently (Mercure et al. 2008).

The face processing area in the ventral temporal cortex is part of the brain network supporting social cognition in humans and other primates. The present study investigated the competing hypotheses outlined above by measuring minicolumn width and cell size asymmetries in the fusiform cortex. It was considered that such asymmetries may be unique to

humans and therefore it was predicted that measurements of minicolumn width and neuron size may reveal a species difference. The mid-fusiform region (roughly equivalent to Brodmann area 37 in human brain) was examined.

Materials and methods

Tissue

Formalin fixed brain tissue was sampled from 14 humans who had died between the ages of 2 and 69 years and 14 chimpanzees with an age range from 1 year to late adulthood (although precise age was only available for four of the youngest animals, including the 1-year old; Table 1). The human brains came from the Thomas Willis Oxford Brain Collection (TWOBC) and the chimpanzee materials were drawn from the comparative brain collection at the Mount Sinai School of Medicine (MSSM, Dr P.R. Hof), New York. Chimpanzee tissue came from subjects that died natural deaths at zoological facilities. Human cases were free from neurological or psychiatric diseases and no alcohol or illegal drug misuse was detected in our sample's medical records. The humans were selected to represent an age range across the lifespan below 70 years old, to avoid severe ageing effects that are more pronounced in the left hemisphere (Di Rosa et al. 2009) and avoiding very elderly subjects who would be far beyond the approximate age range of the chimpanzee materials. The chimpanzee specimens were drawn from a larger collection for which the age range spanned from 1 to 57 years old and the materials included in this study represent a random sample from approximately this range. Age matching was not possible because accurate chimpanzee ages were not available for all cases. Collection and preservation of chimpanzee brains is less standardised than for human brains and precise post-mortem interval was not recorded but was within 30 h of death. The brain weight and handedness of chimpanzees in this study were unknown. Apart from the 1- and 2-year-old animals, none of the other chimpanzee tissue had the appearance of either extreme of the age range (neither characteristically immature in appearance nor showing signs of atrophy associated with old age). Specimens included a mix of male and female animals and the tissue was long fixed with post-mortem intervals comparable to the human subjects, showing no evidence of brain pathology.

For the human materials, demographic details and potentially confounding variables, including age at death (mean 31 years, SD 22.7), fixation time (mean 153.3 months, SD 91.4) and post-mortem interval (mean 48.8 h, SD 26.3) were subjected to statistical analysis (see below). Hand preference for humans and chimpanzees was unknown. Mean fresh brain weight for humans was

Table 1 Age and sex for subjects that are known

Specimen	Age	Sex
Chimpanzee01	1	Female
Chimpanzee02	2	Female
Chimpanzee03	6	Male
Chimpanzee04	11	Male
Chimpanzee05	N/A	Female
Chimpanzee06	N/A	Female
Chimpanzee07	N/A	Female
Chimpanzee08	N/A	Male
Chimpanzee09	N/A	N/A
Chimpanzee10	N/A	N/A
Chimpanzee11	N/A	N/A
Chimpanzee12	N/A	N/A
Chimpanzee13	N/A	N/A
Chimpanzee14	N/A	N/A
Human01	2	Male
Human02	2	Female
Human03	8	Female
Human04	13	Male
Human05	16	Male
Human06	21	Female
Human07	25	Male
Human08	26	Female
Human09	35	Female
Human10	41	Female
Human11	56	Male
Human12	57	Female
Human13	61	Female
Human14	69	Female

N/A not available

1,390.1 g (SD 151.9). All tissue was assigned a randomised code so that measurement proceeded blind to case identity, hemisphere and species (although species was often apparent from the appearance of the tissue). The brains were photographed during dissection to aid localisation.

Tissue sampling

The region of interest (ROI) was the mid-fusiform cortex (in humans: equivalent to Brodmann area 37) on the inferior surface of the temporal lobe. Five-mm-thick coronal blocks of temporal cortex were cut orthogonal to the long axis of the gyrus. The slice cuts began effectively random with respect to the ROI boundary and a random 5-mm-thick block was removed from within the ROI. The mid-fusiform cortex was identified on the inferior surface of the temporal lobe, lying medial to the inferior temporal gyrus, approximately parallel to the posterior limit of the hippocampus. In human brain, area 37 lies posterior to area 20

and anterior to the ventral portion of area 19, and was delineated within the fusiform gyrus, bounded laterally by the occipitotemporal sulcus and medially by the collateral sulcus. Structural landmarks were used to help to determine the anterior limit, defined by the midline ventral splenium of the corpus callosum, and the posterior limit defined by the parasplenial posterior cingulate sulcus (Fig. 1). In chimpanzee brain the selection of the ROI was based on sulco/gyral pattern, which is similar between chimpanzees and humans and on landmarks including the hippocampus, the corpus callosum and cingulate cortex. Chimpanzees have a clearly developed fusiform region enabling structural comparison, unlike some other primates such as the macaque monkey. While some cytoarchitectonic maps do not include area 37/PH in all primate species, the ROI definition here was informed by the fMRI localisation of face processing in chimpanzees reported by Parr et al. (2009). Comparative studies acknowledge that “there is no perfect correlation of physiologically neuronographic areas with cytoarchitectural areas” (Bailey et al. 1950). However, Parr et al. (2009) demonstrated that chimpanzees utilise the same mid-fusiform region homologous to that of the human brain. In addition to the macroscopic definition, structural homology was also based on the cytoarchitecture and immunohistochemistry described below.

For sectioning, the blocks were cryoprotected by immersion in a 30 % sucrose solution, periodically refreshed, for 4 weeks, then frozen, and stored at -80°C . A cryotome was used to cut 30- μm -thick frozen sections for slide mounting. For image analysis four sections per case were assessed—two sections were selected from each hemisphere, spaced to preserve the systematic-random nature of the sample so that the entire ROI had a chance of being sampled.

Cytoarchitecture

Although the precise location of the fusiform face area (FFA) is variable among individuals and cannot be confirmed without *in vivo* fMRI analysis, to our knowledge there is no such collection of brain tissue available. However, area 37 is the classical location for the FFA in human brain (e.g., see Gathers et al. 2004) from brain imaging studies and therefore represents the best neuroanatomical estimate of its location.

The cytoarchitectonic descriptions of von Economo and Koskinas (1925) were used as a guide. Area PH (anteriorly, subregion PH_T, and posteriorly, subregion PH_O) approximately corresponds to the area 37 identified by neuroimaging studies. Cytoarchitectural characteristics, although variable, include generally small cells with relatively high density overall, fine radial minicolumns, clear and wide granular layers, merging of layers V and VI, a distinct white matter border, and above average cortical thickness.

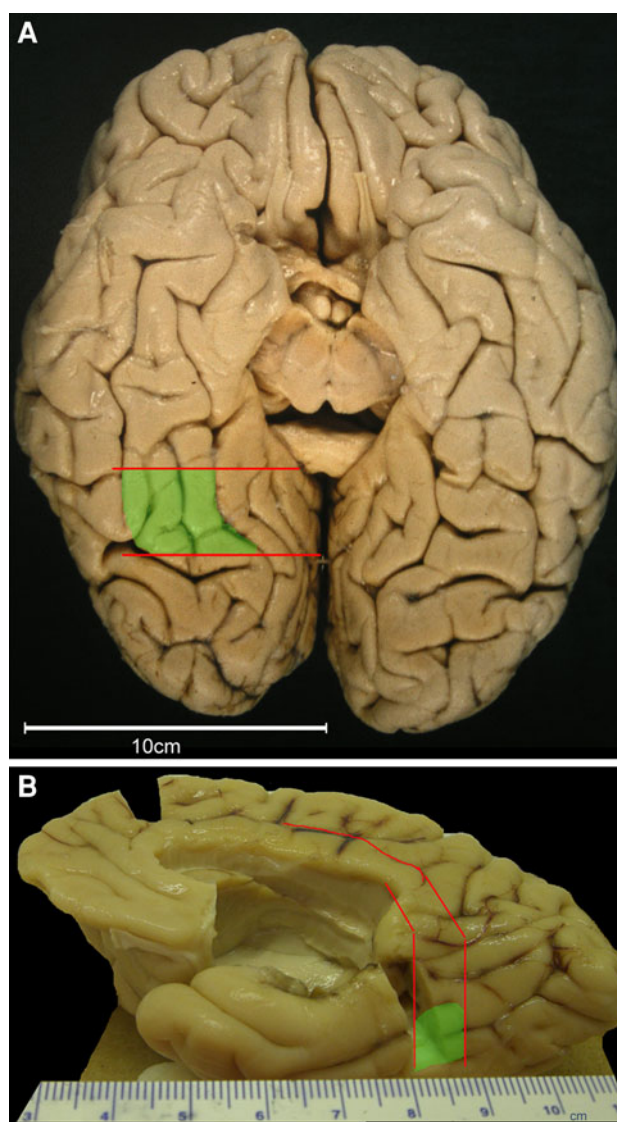


Fig. 1 Macroscopic localisation of regions of interest in human (a, ventral surface of brain) and chimpanzee (b, ventromedial view of brain) brains. In a, the right hemisphere ROI (green region) is identified in the fusiform gyrus delimited between the anterior limit (red line) defined by the midline ventral splenium of the corpus callosum and the posterior limit (red line) defined by the parasplenial posterior cingulate sulcus. In b, a chimpanzee brain with a 5-mm-thick block removed from the ROI (green region) between lines determined by the equivalent landmarks (red straight lines), with part of the posterior cingulate sulcus traced to its most posterior point in red. (Some additional structures; a block of prefrontal cortex, thalamus, and midline corpus callosum have been dissected from the chimpanzee brain, which were generally not fully intact in the available brain collection). See main text for cytoarchitectural descriptions

Anteriorly, area TE (equivalent to area 20) has more sparse cells in layers II and III which are less rigidly columnar, the granular layer IV is looser and more split into columns and layers V and VI tend to be more separable than in PH with more dense, larger cells. The contrasting region posteriorly

is area OA (equivalent to area 19), wherein layers II and III have a more similar width and appear more merged, layer V is relatively light with small cells, while layer VI has a stronger band of larger cells, and radial minicolumns tend to be clearer in the lower layers. In chimpanzees the regional pattern is similar although, the size of cells was smaller, the depth of cortex was less and the density of cells was greater (see Fig. 2). For chimpanzee material, the dissection was carried out at the comparative brain bank at the Mount Sinai School of Medicine, New York. In absolute size the ROI in chimpanzee brains is smaller than that of humans due to smaller overall brain size.

The fusiform cortex was clearly visible and preserved in the whole width on the sections studied. Consistency of measurements from different locations within the same ROI was good and more similar within cases than between cases, indicating relative homogeneity of the region sampled in both humans and chimpanzees (see also reliability and accuracy section below).

Tissue staining

Cresyl violet staining of Nissl bodies in cell cytoplasm was performed to visualise cell bodies for the quantitative analysis of minicolumns and cell morphology. Sections were de-fatted in 100 % alcohol hydrated in successively decreasing alcohol solutions, stained with 0.1 % cresyl violet solution (0.5 g cresyl violet, 500 ml distilled water, 4-ml 10 % acetic acid) for 2 min and then dehydrated in successively increasing alcohol solutions (70, 95, 100, 100 %). The sections were then cleared in two changes of xylene and coverslipped with DPX.

Although it was not deemed appropriate for quantitative assessment in these materials, immunohistochemistry was used to observe qualitative cytoarchitectural similarity of the regions of interest in the two species (Fig. 3). Antibodies to neurofilament proteins, SMI32 (Covance, Princeton, New Jersey, USA; product SMI-32P-100) and N200 (Sigma, Gillingham, UK; product N0142-2ML) were used. The labelling was comparable with previous data from macaques, humans (Hof and Morrison 1995; Law and Harrison 2003), and chimpanzee (Sherwood et al. 2007). Antigen retrieval techniques were used on 10- μ m-thick sections. For human tissue the optimal concentrations were 1:400 for SMI-32 and 1:1,000 for N200. For chimpanzee tissue the optimal concentrations were 1:100 for SMI-32 and 1:800 for N200.

Image analysis

Minicolumn width

Minicolumn width was quantified using semi-automated image analysis. The method has been reported in detail

with stereological validation, illustration, and discussion of assumptions (Buxhoeveden et al. 2000; Casanova and Switala 2005; Chance et al. 2006; Di Rosa et al. 2009). For measurements, two sections containing each ROI provided an adequate sample (a mean of 108 minicolumns were sampled per ROI, with consistency between slides within the same ROIs (Pearson's correlation = 0.94, $p < 0.01$, and overall coefficient of error < 0.1). Minicolumn detection was optimised for layer III, where minicolumns are clearest. In summary, layer III was photographed through a 4 \times objective lens, normal to the cortical surface, and the photomicrographs were digitised at 0.4- μ m/pixel resolution. Three micrographs were captured from each ROI, each micrograph comprising a region approximately 1 mm² in area. Fields were selected in a random grid pattern excluding the regions of highest cortical curvature at the fundi of sulci and the apices of gyri where high curvature affects cell distribution [although minicolumns are still clearly visible (Chance et al. 2004)].

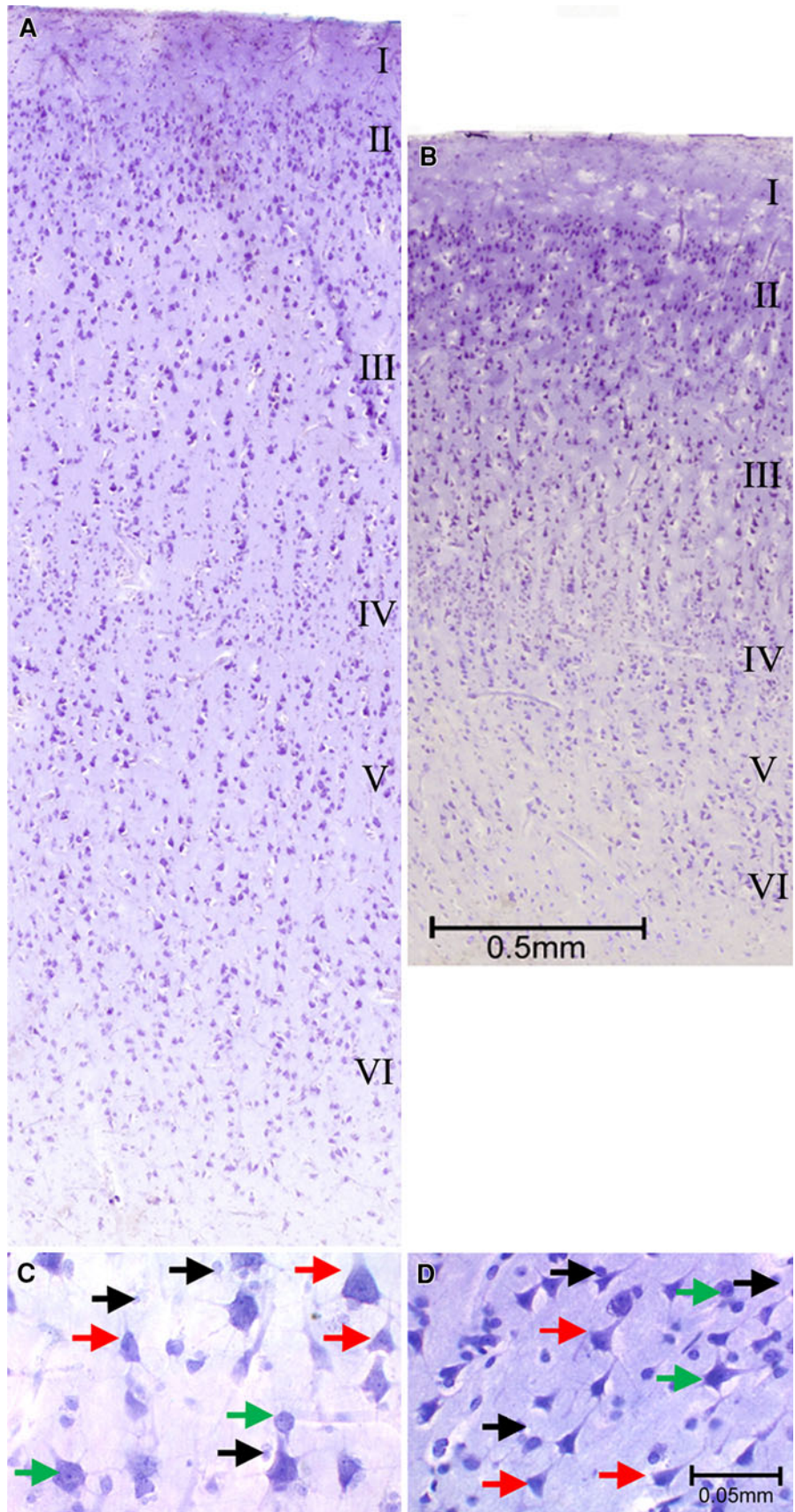
As defined here, minicolumn width is a single value calculated from the combined width of the cell dense core plus the sum of the two halves of the peripheral neuropil (where synapses and dendrites predominate) on either side. The software automatically segments the images to select neurons. Measurements of clustering are applied to determine the periodicity of columnar distribution. The method has been modified from a previous version of the program (Buxhoeveden et al. 2001) to take better account of incomplete minicolumns aligned imperfectly with the surface of the section (Di Rosa et al. 2009). A minicolumn segment was required to contain at least 10 aligned neurons. This minimum definition is similar to reports that a minimum of 8 neurons is found per minicolumn-sized area (Buldyrev et al. 2000) and the maximum number of Nissl-stained neurons, typically arranged into columns, ranges from 15 to 22 (Gabbott 2003).

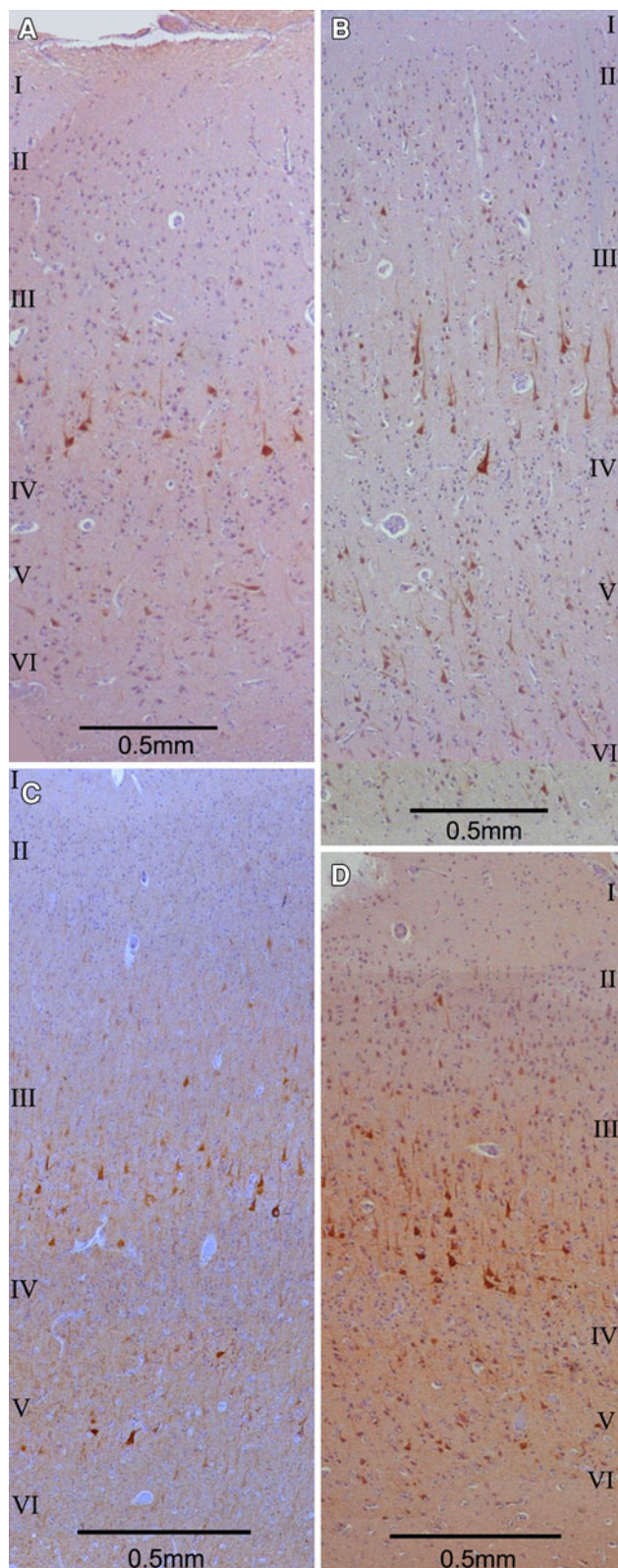
The potential confounding effects of over-projection and lost caps are limited by use of a sectioning thickness (30 μ m) that approximates a single plane of columns and by ignoring minicolumn fragments with fewer than 10 cells. Frozen sections provide conserved x , y dimensions and measurement of section thickness (minimum 12.2 μ m) indicated approximately 60 % z -axis collapse. Compression in the z -direction potentially benefits the 2-dimensional minicolumn analysis. Random variance in alignment between sections is minor compared to the inter-subject differences that are of interest: across all cases, fields of view from non-contiguous sections within the same fusiform gyrus reveal a Pearson's correlation of 0.94 ($p < 0.01$).

Cell density

Samples were visualised using an Olympus BH-2 photomicroscope with a 40 \times objective lens connected to a PC

Fig. 2 Mid-fusiform (Brodmann's area 37) cortical layers in a 41-year-old human (**a**) and a chimpanzee (~45-year old) (**b**). The depth of the cortex in both species is variable. Nissl staining of layer III neurons and glia from a human (**c**) and chimpanzee (**d**). *Red arrows* indicate pyramidal neurons, *yellow arrows* indicate non-pyramidal neurons, *black arrows* indicate glial cells. Image contrast has been slightly improved for illustration. Images **a** and **b** are at the same scale (*scale bar shown in b*), images **c** and **d** are at the same scale (*scale bar shown in d*)





◀ **Fig. 3** Composite images of immunohistochemical staining for neurofilament-containing cells: N200 (**a**, **c**) and SMI-32 (**b**, **d**). **a** and **b** Sections from the same human brain and **c** and **d** are sections from the same chimpanzee brain. Humans and chimpanzees show similar cytoarchitectural patterns: for both antibodies staining is seen in layers III and V. For N200, the majority of immunolabelled neurons were found in lower layer III, and in both humans (**a**) and chimpanzees (**c**) usually one, or occasionally two, pyramidal neurons in a minicolumn were immunoreactive. For SMI-32, stained neurons in layer III were spread more widely, often with several immunoreactive cells within a minicolumn. In the human (**b**) and chimpanzee (**d**) examples can be seen with at least five stained neurons in a single minicolumn within layer III. Image contrast has been slightly improved for illustration. Images **a** and **b** are at the same scale, images **c** and **d** are at the same scale

were positioned at regularly spaced intervals throughout layer III using a randomly oriented grid coordinate system. The counting frames used the standard stereological procedure of two inclusion edges and two exclusion edges. Cells were counted through a depth of 10 μm ensuring a minimum guard zone of 1 μm above and 1 μm below (larger in most cases due to additional final z thickness). In humans, an average of 264 neurons (minimum 192) and 155 glial cells (minimum 124) were counted within layer III of each hemisphere. In chimpanzees, means of 362 neurons (minimum 214) and 151 glial cells (minimum 92) were counted. For each brain, mean density per mm^3 was calculated for each cell type.

Pyramidal neurons, non-pyramidal neurons and glial cells were categorised based on Nissl stain pattern (Fig. 1c, d). All neurons have a distinct nucleus and darkly stained nucleolus, surrounded by lighter stained dendritic process. Pyramidal neurons are distinguished from non-pyramidal neurons by their “teardrop” shape with prominent apical dendrite. Glial cells tend to have invisible cytoplasm with no nucleolus and a thicker nuclear membrane than neurons, with more spots of dark chromatin, particularly near the nuclear membrane. Consistent with previous studies (Sherwood et al. 2006) glia were not further sub-divided into astrocytes or oligodendrocytes, and identifiable microglia were excluded.

Cell size

Size of pyramidal neurons, non-pyramidal neurons and glia was also assessed with a 40 \times objective lens. All cells counted within the counting frame were outlined from which the cross-sectional area of each cell was computed. Neurons were outlined when they had an in-focus nucleolus so that the maximum area of each neuron was measured, counter-acting the bias toward sampling large cells more often.

computer, running KS 400 3.0 image analysis software (Imaging associates, Bicester, UK). For systematic random sampling, counting frames (area per frame: 6,690 μm^2)

Reliability and accuracy

In 10 randomly chosen subjects (5 humans, 5 chimpanzees) measurements of cell density and cell size were repeated for one hemisphere. Strictly parallel, single measure, intra-class correlation coefficients for absolute agreement were used to test the repeatability of mean estimates per subject. Values were pyramidal neuron density 0.85, non-pyramidal neuron density 0.94, glial density 0.79, pyramidal neuron size 0.93, non-pyramidal neuron size 0.78 and glial cell size 0.83, indicating good reliability of measurements (all had a $p < 0.005$). Measurements of apparent somatic areas were also repeated on a further 10 saved images to check cell boundary and area estimation on identical cells. These yielded a Pearson's correlation of 0.96 for pyramidal neurons, 0.95 for non-pyramidal neurons and 0.91 for glia, indicating good reproducibility. All coefficients of error for all measured variables of interest (minicolumn widths, cell densities and cell sizes) were between 0.01 and 0.1, indicating good accuracy of measurements (<0.1 is desirable).

Statistical analysis

Statistical analyses were conducted using SPSS software (version 17.0). Measured variables were tested to determine if they met the conditions for parametric analyses. All data in each species passed Kolmogorov–Smirnov tests indicating a normal distribution. Pyramidal neuron density, pyramidal neuron cross-sectional area and non-pyramidal neuron cross-sectional area also passed Box's *M*-tests for homogeneity of variance and, consequently, were analysed by repeated measures analysis of variance (rmANOVA, which tests differences between and within subjects). Glial cell density, glial cell area, non-pyramidal neuron density and minicolumn widths did not pass Box's *M*-test, therefore these were analysed with Mann–Whitney *U* tests for each hemisphere separately.

Hemispheric asymmetries of all data were calculated as $[(\text{left} - \text{right})/\text{mean}] \times 100$, yielding, for example, the size difference between pyramidal cells in the two hemispheres as a percentage of the mean pyramidal cell size. All of these asymmetry measures passed the tests for normal distributions and homogeneity of variance and so were subjected to *t* tests.

Imprecise information on the chimpanzee demographic data, including age at death, post-mortem interval (PMI), fixation time, total brain size and sex in several specimens, meant that these data could not be included as covariates or analysed for species differences. Consequently, age adjustment relative to the species' lifespans (presumably a non-linear function) was not attempted. In humans, the demographic covariate data and its relationship to the measured variables were assessed by Pearson's correlation

analysis and *t* tests as described in the “**Results**” section. Details of the results are reported as *F*-statistics, *t*-statistics, *U*-statistics or r^2 coefficients as appropriate. In order to aid intelligibility, statistical details are confined to positive results and negative results that may be considered trends or demonstrate an important negative.

Methodological limitations

It should be noted that this study cannot satisfy stereological requirements fully as the identification of fusiform cortex anatomy and minicolumnar organisation requires a non-random orientation of tissue (i.e., a parallel slice design). Furthermore, the 3-dimensional curvature of the region limits the identification of cortical layers if randomly orientated (Dorph-Petersen et al. 2007). All of the tissue in this study had been stored in formalin for longer than the 3–6 weeks required for shrinkage to stabilise (Quester and Schroder 1997).

Results

Tables 2 and 3 describe data summary and statistical analysis summary, respectively.

Minicolumn width

Minicolumns in both hemispheres were approximately 30 % wider in humans than in chimpanzees. There was a species difference in the asymmetry of minicolumn width: humans were significantly asymmetrical (the asymmetry value was different from zero), with wider minicolumns in the left hemisphere compared to the right hemisphere (see Tables 2 and 3, and discussion below). By contrast, there was no difference between the hemispheres for chimpanzee minicolumns (Fig. 4).

Cell size (cross-sectional area)

Pyramidal neuron mean cross-sectional area was approximately 35 % smaller in chimpanzees compared to humans. Humans had a significant asymmetry due to larger pyramidal neurons in the left hemisphere (about 8 % larger than the right), whereas chimpanzees were not asymmetrical (Fig. 4). Non-pyramidal neurons were similar in both species. Although mean size was smaller in chimpanzees (see Table 2), this was not a significant difference. There was no hemisphere difference in either species and no difference between species. Glial cells were slightly larger in chimpanzees compared to humans, in both hemispheres. There was no asymmetry and no species difference of asymmetry.

Table 2 Means and standard deviations of measured variables for the left and right hemispheres

Species	Minicolumn width (μm)		Pyramidal neuron density (mm^{-3})		Non-pyramidal neuron density (mm^{-3})		Glial cell density (mm^{-3})		Pyramidal neuron size (μm^2)		Non-pyramidal neuron size (μm^2)		Glial cell size (μm^2)	
	Left	Right	Left	Right	Left	Right	Left	Right	Left	Right	Left	Right	Left	Right
Human ($N = 14$)	35.23 \pm 2.96	33.74 \pm 1.47	13.897 \pm 2.857	14.904 \pm 3.031	14.769 \pm 2.694	14.818 \pm 1.574	17,025 \pm 2,910	17,270 \pm 3,267	176.5 \pm 26.2	162.7 \pm 25.6	75.7 \pm 8.6	73.6 \pm 7.7	16.5 \pm 1.75	16.3 \pm 2.5
Chimpanzee ($N = 14$)	26.04 \pm 3.00	26.32 \pm 3.48	23.534 \pm 5.330	23.502 \pm 5.725	26.669 \pm 7.341	29.256 \pm 9.216	21,028 \pm 5,011	21,936 \pm 8,435	110.2 \pm 20.8	112.5 \pm 23.0	69.1 \pm 12.1	68.9 \pm 14.9	19.6 \pm 4.2	19.9 \pm 4.0

Cell density

Pyramidal neuron density was higher in chimpanzees than humans. There was no hemispheric asymmetry. Although the mean density was lower on the left than the right in humans (Table 2) this was not a significant asymmetry and the more symmetrical chimpanzee data did not result in a species difference (Table 3). Non-pyramidal neurons were denser in humans compared to chimpanzees. There were no asymmetries revealed by calculation of the interhemispheric asymmetry values or differences of asymmetry between species. (Although the mean values for non-pyramidal neurons appear asymmetric in chimpanzees the high variance limits confidence in the estimate of the true mean and there was no significant asymmetry revealed by within subject testing.) Glial cells were denser in chimpanzees compared to humans for the left hemisphere but there was no species difference for the right hemisphere (mainly due to relatively high variance in the chimpanzee data). There were no asymmetries or differences of asymmetry between species.

Immunohistochemistry

The staining patterns of SMI-32 and N200 antibodies were similar in the two species. This cytoarchitectural similarity supports the notion of regional homology of the ROIs between the species. The SMI-32 staining identified pyramidal neurons in the bottom and middle regions of cortical layer III and slightly less prominently in layer V. By contrast the N200 staining identified fewer cells, also mainly pyramidal neurons, usually confined to the bottom of layer III as well as in layer V. In both humans and chimpanzees the wider distribution of SMI-32-immunoreactive neurons within layer III often stained multiple neurons within the same minicolumn (Fig. 3b, d), whereas this was rarely the case for N200 staining (Fig. 3a, c).

Demographic correlates, age and brain size

As described in the “Materials and methods”, accurate demographic data sufficient for analysis was only available for the human sample. PMI and fixation time were not known for the chimpanzees. For the human sample there was no relationship of either PMI or fixation time with any of the measured variables including minicolumns, glia, non-pyramidal and pyramidal cell densities or areas in either the left or right hemisphere. Brain size (whole brain weight in grams) was also not related to any measured variables in humans (notwithstanding an isolated trend for a positive correlation with non-pyramidal neuron size only in the left hemisphere: $r^2 = 0.59$, $p = 0.06$).

Table 3 Table of statistical results for contrasts between species, hemispheres (hemi) and other interactions

Measurement	Species difference		Hemisphere difference		Further contrasts		
	Statistic	<i>p</i> value	Statistic	<i>p</i> value	Interaction	Statistic	<i>p</i> value
Mimicolumns							
Mimicolumn width	(Mann–Whitney) Left hemi: $U = 0$, $Z = -0.45$; Right hemi: $U = 3.0$, $Z = -4.40$	Left hemi: <0.01 ; Right hemi: <0.01	–	–	–	–	–
Hemispheric asymmetry value (post hoc)	$t_{(26)} = 2.33$	<0.05	Human: $t_{(13)} = 2.6$ Chimpanzee: $t_{(13)} = -0.6$	Human: <0.05 Chimpanzee: 0.56	–	–	–
Cell density							
Pyramidal neuron density	(rmANOVA) $F_{(1,26)} = 33.15$	<0.01	(rmANOVA) $F_{(1,26)} = 0.91$	0.35	NS	NS	NS
Asymmetry value (post hoc)	$t(26) = -1.36$	0.19	NS	NS	–	–	–
Non-pyramidal neuron density	(Mann–Whitney) Left hemi: $U = 8.0$, $Z = -4.14$; Right hemi: $U = 6.0$, $Z = -4.23$	Left hemi: <0.01 ; Right hemi: <0.01	–	–	–	–	–
Asymmetry value (post hoc)	NS	NS	NS	NS	–	–	–
Glial cell density	(Mann–Whitney) Left hemi: $U = 45.0$, $Z = -2.44$; Right hemi: $U = 71.0$, $Z = -1.24$	Left hemi: <0.05 ; Right hemi: 0.23	–	–	–	–	–
Asymmetry value (post hoc)	NS	NS	NS	NS	–	–	–
Cell size (cross-sectional area)							
Pyramidal neuron size	(rmANOVA) $F_{(1,26)} = 46.11$	<0.01	(rmANOVA) $F_{(1,26)} = 3.78$	0.06	Species X hemisphere	$F_{(1,26)} = 7.38$	0.01
Hemispheric asymmetry value (post hoc)	$t_{(26)} = 2.25$, $p < 0.05$	<0.05	Human: $t_{(13)} = 3.32$, Chimpanzee: $t_{(13)} = -0.47$	<0.01 0.65	–	–	–
Non-pyramidal neuron size	(rmANOVA) $F_{(1,26)} = 2.08$	0.16	(rmANOVA) $F_{(1,26)} = 0.30$	0.59	NS	NS	NS
Hemispheric asymmetry value (post hoc)	$t_{(26)} = 0.33$	0.74	NS	NS	–	–	–

Table 3 continued

Measurement	Species difference		Hemisphere difference		Further contrasts		
	Statistic	<i>p</i> value	Statistic	<i>p</i> value	Interaction	Statistic	<i>p</i> value
Glial cell size	(Mann–Whitney) Left hemi: $U = 48.0$, $Z = -2.30$ Right hemi: $U = 45.0$, $Z = -2.44$	Left hemi: <0.05 ; Right hemi: <0.05	NS	NS	–	–	–
Hemispheric asymmetry value (post hoc)	$t_{(26)} = 0.72$	0.48	NS	NS	–	–	–

For each variable the main test is reported (either repeated measure ANOVA (mANOVA) or Mann–Whitney *U*) and additional post hoc *t* tests on the asymmetry measure derived from that variable are also reported. The table shows significant effects ($p > 0.05$), trends ($p > 0.05$ and <0.1) and non-significant findings of interest, which are referred to in the text. All other contrasts showed no significant or trend effects ($p \geq 0.1$) reported as ‘NS’)

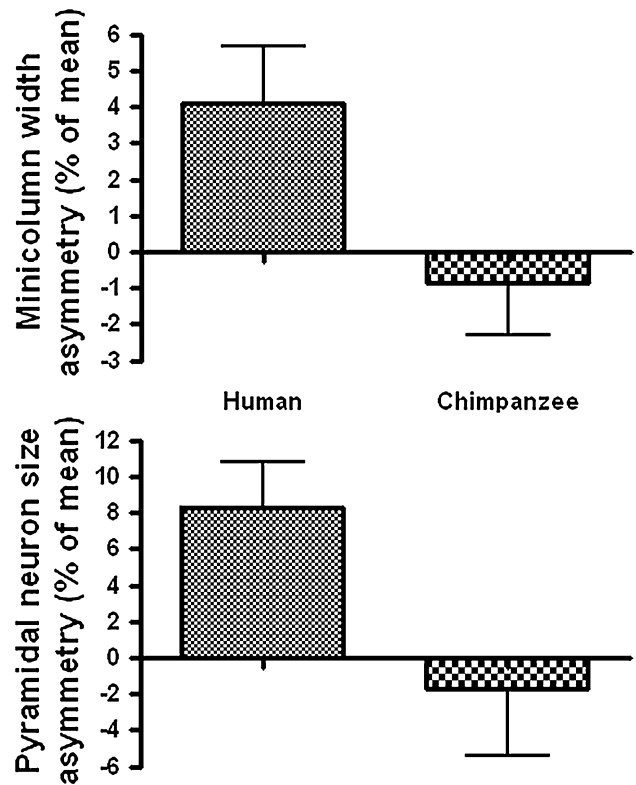


Fig. 4 Significant leftward asymmetry of human minicolumn width and pyramidal neuron size ($N = 14$ humans and 14 chimpanzees). Chimpanzees have no asymmetry, and the species contrast is significant ($p < 0.05$) for both measurements. See “Materials and methods” for details

Age was only known for four chimpanzees and therefore was insufficient for analysis. For humans there was a clear tendency for older individuals to have smaller neurons. Pyramidal neuron cross-sectional area was negatively correlated with age for both the left ($r^2 = -0.71$, $p < 0.01$) and right ($r^2 = -0.76$, $p < 0.01$) hemispheres. Left hemisphere non-pyramidal neurons were also smaller in older subjects ($r^2 = -0.63$, $p < 0.05$). Although the relationship between minicolumn width and age was negative, as expected, the correlation was not significant for either the left hemisphere ($r^2 = -0.14$, $p = 0.63$) or the right hemisphere ($r^2 = -0.22$, $p = 0.44$).

Sex was known for eight chimpanzees (5 females, 3 males) so the data were cursorily tested for sex differences. There were no sex differences for any of the measured cellular and minicolumn variables in the chimpanzees. In humans there were no gender differences for any of the measured variables, nor for age, fixation or PMI. However, women’s brains weighed less than men’s brains ($t = -2.68$, $df 9$, $p < 0.03$), reflecting the typical gender difference in human brain size.

Discussion

Three main findings emerge from this study of fusiform cerebral cortex: (1) in general, the neurons are larger and the spacing between them is greater in humans compared to the chimpanzee, (2) minicolumns are wider in the left hemisphere compared to the right in humans, but are not asymmetric in chimpanzees, (3) pyramidal neurons are larger in the left hemisphere compared to the right in humans, but are not asymmetric in size in chimpanzees. The three observations present a coherent picture; that cells have become or remained large and less densely packed in the evolution of human mid-fusiform cortex (area 37, the approximate location of the face processing area), compared to the chimpanzee, and that this is accentuated in the left hemisphere to generate an inter-hemispheric asymmetry. To our knowledge, no previous studies have made similar histological comparisons in the human and chimpanzee fusiform gyrus.

The present findings were striking in two respects: first, the wider minicolumns and larger neurons were not found in the hemisphere dominant for face perception, and second, a statistically significant species difference in neuro-anatomical asymmetry was found even though the functional species difference in face processing is much less clear than it is for language. The mid-posterior ventral fusiform processes visual objects in humans, chimpanzees and other primates. The asymmetrical specialisation of sub-fields such as the FFA or visual word form area arises from expertise in certain sub-categories of visual object. We consider that structural asymmetry in this region may be related to these known asymmetrical functions.

Two functions may correspond to a structural asymmetry in fusiform cortex: face perception [which is not clearly lateralized in chimpanzees (Parr et al. 2009)], and word recognition (Moore and Price 1999; Greenblatt 1990) (which is a characteristically human behaviour). However, the visual word form area is usually identified in a location posterior to the area examined in this study. Nonetheless, recent research shows that better literacy enhances left fusiform activation inducing competition with face processing in that area while also enhancing phonological activation in the planum temporale (Dehaene et al. 2010). The interaction suggests a network effect in these regions which may be influenced by the acquisition of language skills.

Dissimilarities between face processing mechanisms in the two species may also contribute to the structural contrast. Although both species perceive faces holistically (see Taubert and Parr 2010, among others, for use of the term holistic and its elucidation in chimpanzee face perception), this process is clearly lateralised in humans—individual facial features are detected in the left hemisphere whereas

holistic analysis is biased to the right hemisphere (Rossion et al. 2000). By contrast, although there is some evidence of right hemisphere activation for visual object processing in chimpanzees it is not specialised for faces as it is in humans (Parr et al. 2009). Reports of lateralisation in another primate species, the rhesus macaque, are also not conclusive (e.g., Pinsk et al. 2005, but see Tsao et al. 2008). Furthermore, claims for lateralised face processing in sheep have depended on indirect methods (e.g., post-mortem RNA measures; see Broad et al. 2000) and response latency but do not show greater face selectivity or larger populations of face cells in the right hemisphere (Peirce and Kendrick 2002). Nonetheless, the present study does not demonstrate that humans are unique in having a right hemisphere bias, only that humans have a corresponding asymmetric minicolumn organisation distinct from their closest primate relative, the chimpanzee.

Although the human minicolumn asymmetry is not large (a little over 4 %) it is consistent with other studies of human minicolumn asymmetry in the planum temporale (Buxhoeveden et al. 2001; Hutsler 2003; Chance et al. 2006). The asymmetry appears to be relatively confined to the mid-posterior fusiform region, as a previous study that included the entire anterior area 20 reported that minicolumn width in human control subjects was non-significantly larger in the right hemisphere (Di Rosa et al. 2009). It should also be noted that the minicolumn width measure is a 2-dimensional measure. Information about the 3-dimensional distribution of minicolumns has indicated a hexagonal distribution across the cortical surface (e.g., Gabbott 2003), although more recent studies suggest greater variability due to less regular polygons (Skoglund et al. 2004). For the purpose of estimation, if the asymmetry of minicolumn width is simplified to a hexagonal distribution (see Chance et al. 2006) this would be expected to account for approximately 9 % asymmetry of surface area. The asymmetry of pyramidal neuron density (a 3-dimensional measure) in humans was only a little less at 7 %.

It is striking that wider minicolumns were not found in the hemisphere usually dominant for face processing. This suggests that minicolumn width is dissociated from dominance and instead relates to the type of processing: featural or holistic. Hemispheric dominance may consequently be determined by which type of processing is dominant for a given function. Greater spacing of minicolumns results in less overlapping dendritic trees and it has been suggested that this allows more independent minicolumn function (Seldon 1981a, b). In general, the wider spacing of minicolumns is associated with wider basal dendrites (Seldon 1981a, b) and we have found that a wider cell dense core is associated with wider peripheral neuropil space (Chance et al. 2006). However, although Seldon (1981a, b) found that the length of basal dendrites of pyramidal cells was

greater in the left hemisphere, this was not sufficient to compensate for hemispheric difference in columnar spacing. The consequence appears to be less overlapping dendritic fields in the hemisphere with wider minicolumn spacing (Hutsler and Galuske 2003). This is hypothesised to create a different computational emphasis between the hemispheres (Harasty et al. 2003).

Harasty et al. (2003) have proposed that widely spaced minicolumns function as discrete units facilitating computational processing of more independent components whereas narrow minicolumns permit greater coactivation and therefore confer more holistic processing. Structurally, their model suggests an inverse relationship with cortical thickness, associating lateral expansion (wide minicolumns) with thin cortex. Jung-Beeman (2005) has characterised the difference in terms of the density of synapses and the distribution of dendritic branches in relation to the cell body, whereby the basal dendrites of right hemisphere pyramidal neurons have longer initial branches and more synapses further from the soma than left hemisphere neurons where the more widely spaced minicolumns have more dendritic branching within their territory. Wider minicolumn spacing is therefore associated with higher resolution processing across less overlapping basal dendritic fields whereas narrow minicolumn spacing is associated with lower resolution, holistic processing due to relatively greater distal sampling of more overlapping fields (Jung-Beeman 2005). Here, we suggest that holistic, configural processing for face recognition benefits from the computational overlap generated by narrow minicolumns in the fusiform gyrus. This mechanistic interpretation is consistent with a correspondence between the rightward lateralisation of holistic face processing and the narrow minicolumns found here in the right hemisphere in humans. The absence of asymmetry in chimpanzees may relate to better performance than humans in tasks such as rapid visuospatial processing and inverted face recognition that have ecological validity for chimpanzees (Matsuzawa 2007).

Different components of face processing (recognition, categorisation, familiarity, facial features) are partially separable and may be subject to differing degrees of lateralisation and specialisation between species. (Wilson and Diaconescu 2006; Young and Yamane 1992). Intact functioning of at least one of these components in humans is linked to minicolumn organisation: human patients with autism have a selective deficit in perceiving facial expressions categorically (Teunisse and De Gelder 2001) which affects activation of the fusiform gyrus (Pierce et al. 2004), and one of the few neuropathological features of the disorder is altered minicolumn organisation (Casanova et al. 2006) accompanied by altered neuron density in layer III of the fusiform gyrus (Van Kooten et al. 2008). The high heritability of face processing (Zhu et al. 2010) makes

it plausible that the neuroanatomical correlate is detectable. Some functional aspects of face processing also change with age—face discrimination ability is reduced in old age (an effect described as “dedifferentiation”; Goh et al. 2010)—and marked minicolumn thinning has been found in fusiform cortex in old age (Di Rosa et al. 2009).

Although the function of minicolumns is not known, age-associated cognitive impairment in rhesus monkey is correlated with regional disruption of minicolumn structure (Cruz et al. 2009). The vulnerability of minicolumns to disruption in old age and dementia (Chance et al. 2011) may be related to the observation here that SMI-32 immunohistochemistry frequently stained multiple neurons vertically within the same minicolumn and SMI-32-immunoreactive neurons are thought to be selectively vulnerable to Alzheimer’s disease (Hof et al. 1990; Morrison et al. 1987). By contrast, N200 staining did not often identify more than a single neuron in a minicolumn and these cells are thought to be a largely separate population that is relatively resistant to Alzheimer’s disease (Radenahmad et al. 2003; Law and Harrison 2003).

In summary, we suggest that the cytoarchitectural asymmetry of human fusiform cortex, and its absence in chimpanzees, reflects a functional difference between the species. The dependence on holistic analysis of faces in both species is consistent with the uniformity of operation of relatively narrow minicolumns found both in chimpanzees and in the right hemisphere of humans. By contrast, the wider minicolumns and larger pyramidal neurons in the human left hemisphere are comparable to the asymmetries found in human language areas and may be consistent with a more widespread association with language related function such as word-form processing. Functional interpretations notwithstanding, there is a striking consistency in the species contrast between humans and chimpanzees in the cytoarchitectural asymmetry of fusiform cortex comparable with that found in other language areas.

Acknowledgments We thank Dr. Chet Sherwood for his contribution to discussion of the project and Dr. Joseph Erwin who both helped P.R.H. with the original collection of chimpanzee brain materials at Mount Sinai School of Medicine. The work was supported by a grant from the European Union framework 6 programme: “What makes us human”. S.A.C. was the recipient of a fellowship from Alzheimer Scotland, UK, and a project grant from Autism Speaks, USA. Additional support was provided by the James S. McDonnell Foundation (grant 22002078) to P.R.H.

References

- Amunts K, Schleicher A, Bürgel U, Mohlberg H, Uylings HBML, Zilles K (1999) Broca’s region revisited: cytoarchitecture and intersubject variability. *J Comp Neurol* 412:319–341

- Anderson B, Southern BD, Powers RE (1999) Anatomic asymmetries of the posterior superior temporal lobes: a postmortem study. *Neuropsychiatry Neuropsychol Behav Neurol* 12:247–254
- Annett M (1985) Left, right, hand and brain: the right shift theory. Lawrence Erlbaum Associates Ltd., Hove
- Bailey P, von Bonin G, McCulloch WS (1950) The isocortex of the chimpanzee. University of Illinois Press, Urbana
- Broad KD, Mimmack ML, Kendrick KM (2000) Is right hemisphere specialization for face discrimination specific to humans? *Eur J Neurosci* 12(2):731–741
- Buldyrev S, Cruz L, Gomez-Isla T, Gomez-Tortosa E, Havlin S, Le R, Stanley HE, Urbanc B, Hyman BT (2000) Description of microcolumnar ensembles in association cortex and their disruption in Alzheimer and Lewy body dementias. *Proc Natl Acad Sci USA* 97:5039–5043
- Buxhoeveden DP, Switala AE, Roy E, Casanova MF (2000) Quantitative analysis of cell columns in the cerebral cortex. *J Neurosci Methods* 97:7–17
- Buxhoeveden DP, Switala AE, Litaker M, Roy E, Casanova MF (2001) Lateralization of minicolumns in human planum temporale is absent in nonhuman primate cortex. *Brain Behav Evol* 57:349–358
- Cantalupo C, Hopkins WD (2001) Asymmetric Broca's area in great apes. *Nature* 414:505
- Casanova MF, Switala AE. (2005) Minicolumnar morphometry: computerized image analysis in Neocortical modularity and the cell minicolumn. In: Casanova MF (ed), Nova Biomedical, New York, pp 161–180
- Casanova MF, van Kooten IA, Switala AE, van Engeland H, Heinsen H, Steinbusch HW, Hof PR, Trippe J, Stone J, Schmitz C (2006) Minicolumnar abnormalities in autism. *Acta Neuropathol* 112(3):287–303
- Chance SA, Crow TJ (2007) Distinctively human: cerebral lateralisation and language in *Homo sapiens*. *J Anthropol Sci* 85:153–164
- Chance SA, Tzotzoli PM, Vitelli A, Esiri MM, Crow TJ (2004) The cytoarchitecture of sulcal folding in Heschl's sulcus and the temporal cortex in the normal brain and schizophrenia: lamina thickness and cell density. *Neurosci Lett* 367:384–388
- Chance SA, Casanova MF, Switala AE, Crow TJ (2006) Minicolumnar structure in Heschl's gyrus and planum temporale: Asymmetries in relation to sex and callosal fiber number. *Neuroscience* 143:1041–1050
- Chance SA, Casanova MF, Switala AE, Crow TJ (2008) Auditory cortex asymmetry, altered minicolumn spacing and absence of aging effects in schizophrenia. *Brain*. 131(12):3178–3192
- Chance SA, Clover L, Cousijn H, Currah L, Pettingill R, Esiri MM (2011) Micro-anatomical correlates of cognitive ability and decline: normal ageing, MCI and Alzheimers disease. *Cereb Cortex* 21(8):1870–1878
- Corballis MC (1992) The lopsided ape: evolution of the generative mind. Oxford University Press, New York
- Crow TJ (2000) Schizophrenia as the price that *Homo sapiens* pays for language: a resolution of the central paradox in the origin of species. *Brain Res Rev* 31:118–131
- Cruz L, Roe DL, Urbanc B, Inglis A, Stanley HE, Rosene DL (2009) Age-related reduction in microcolumnar structure correlates with cognitive decline in ventral but not dorsal area 46 of the rhesus monkey. *Neuroscience* 158(4):1509–1520
- Dehaene S, Pegado F, Braga LW, Ventura P, Filho GN, Jobert A, Dehaene-Lambertz G, Kolinsky R, Morais J, Cohen L (2010) How learning to read changes the cortical networks for vision and language. *Science* 330:1359–1364
- Di Rosa E, Crow TJ, Walker MA, Black G, Chance SA (2009) Reduced neuron density, enlarged minicolumn spacing and altered ageing effects in fusiform cortex in schizophrenia. *Psychiatry Res* 166(2–3):102–115
- Dorph-Petersen KA, Pierri JN, Wu Q, Sampson AR, Lewis DA (2007) Primary visual cortex volume and total neuron number are reduced in schizophrenia. *J Comp Neurol* 501(2):290–301
- Gabbott PL (2003) Radial organization of neurons and dendrites in human cortical areas 25, 32, and 32'. *Brain Res* 992(2):298–304
- Gannon PJ, Holloway RL, Broadfield DC, Braun AR (1998) Asymmetry of chimpanzee planum temporale: humanlike pattern of Wernicke's brain language area homolog. *Science* 279(5348):220–222
- Gathers AD, Bhatt R, Corbly CR, Farley AB, Joseph JE (2004) Developmental shifts in cortical loci for face and object recognition. *NeuroReport* 15(10):1549–1553
- Geschwind N, Levitsky W (1968) Human brain: left–right asymmetries in temporal speech region. *Science* 161:186–187
- Goh JO, Suzuki A, Park DC (2010) Reduced neural selectivity increases fMRI adaptation with age during face discrimination. *Neuroimage* 51(1):336–344
- Greenblatt SH (1990) Alexia without agraphia, right homonymous hemianopsia, and color anomia. Report of four cases with location of the lesion by computerized axial tomography of the brain. *Brain Lang* 38(4):576–595
- Harasty J, Seldon HL, Chan P, Halliday G, Harding A (2003) The left human speech-processing cortex is thinner but longer than the right. *Laterality* 8(3):247–260
- Hof PR, Cox K, Morrison JH (1990) Quantitative analysis of a vulnerable subset of pyramidal neurons in Alzheimer's disease: I. Superior frontal and inferior temporal cortex. *J Comp Neurol* 301:44–54
- Hof PR, Morrison JH (1995) Neurofilament protein defines regional patterns of cortical organization in the macaque monkey visual system: a quantitative immunohistochemical analysis. *J Comp Neurol* 352:161–186
- Holloway RL, De LaCoste-Lareymondie MC (1982) Brain endocast asymmetry in pongids and hominids: some preliminary findings on the paleontology of cerebral dominance. *Am J Phys Anthropol* 58:101–110
- Horton JC, Adams DL (2005) The cortical column: a structure without a function. *Philos Trans R Soc Lond B Biol Sci* 360:837–862
- Hutsler JJ (2003) The specialized structure of human language cortex: pyramidal cell size asymmetries within auditory and language-associated regions of the temporal lobes. *Brain Lang* 86(2):226–242
- Hutsler J, Galuske RA (2003) Hemispheric asymmetries in cerebral cortical networks. *Trends Neurosci* 26(8):429–435
- Jung-Beeman M (2005) Bilateral brain processes for comprehending natural language. *Trends Cogn Sci* 9:512–518
- Kanwisher N, McDermott J, Chun MM (1997) The fusiform face area: a module in human extrastriate cortex specialized for face perception. *J Neurosci* 17(11):4302–4311
- Law AJ, Harrison PJ (2003) The distribution and morphology of prefrontal cortex pyramidal neurons identified using anti-neurofilament antibodies SMI32, N200 and FNP7. Normative data and a comparison in subjects with schizophrenia, bipolar disorder or major depression. *J Psychiatr Res* 37(6):487–499
- Matsuzawa T (2007) Comparative cognitive development. *Dev Sci* 10(1):97–103
- McManus IC (1985) Handedness, language dominance and aphasia: a genetic model. *Psychological Medicine, Monograph Supplement* No.8. Cambridge University Press, Cambridge
- Mercure E, Dick F, Halit H, Kaufman J, Johnson MH (2008) Differential lateralization for words and faces: category or psychophysics? *J Cogn Neurosci* 20(11):2070–2087
- Moore CJ, Price CJ (1999) Three distinct ventral occipitotemporal regions for reading and object naming. *NeuroImage* 10(2):181–192

- Morrison JH, Lewis DA, Campbell MJ, Huntley GW, Benson DL, Bouras C (1987) A monoclonal antibody to non-phosphorylated neurofilament protein marks the vulnerable cortical neurons in Alzheimer's disease. *Brain Res* 416:331–336
- Mountcastle VB (1997) The columnar organization of the neocortex. *Brain* 120(4):701–722
- Ono K, Nakamura A, Yoshiyama K, Kinkori T, Bundo M, Kato T, Ito K (2011) The effect of musical experience on hemispheric lateralization in musical feature processing. *Neurosci Lett* 496(2):141–145
- Parr LA, Hecht E, Barks SK, Preuss TM, Votaw JR (2009) Face processing in the chimpanzee brain. *Curr Biol* 19:50–53
- Peters A (2010) The morphology of minicolumns. In: Blatt GJ (ed) *The neurochemical basis of autism: from molecules to minicolumns*. Springer, New York, pp 45–68
- Pierce K, Haist F, Sedaghat F, Courchesne E (2004) The brain response to personally familiar faces in autism: findings of fusiform activity and beyond. *Brain* 127(12):2703–2716
- Peirce JW, Kendrick KM (2002) Functional asymmetry in sheep temporal cortex. *Neuroreport* 13:2395–2399
- Pinsk MA, DeSimone K, Moore T, Gross CG, Kastner S (2005) Representations of faces and body parts in macaque temporal cortex: a functional MRI study. *Proc Natl Acad Sci USA* 102:6996–7001
- Quester R, Schroder R (1997) The shrinkage of the human brain stem during formalin fixation and embedding in paraffin. *J Neurosci Methods* 75:81–89
- Radenahmad N, Neal JW, Wilcock GW, Pearson RCA (2003) A neurofilament antibody recognises a subset of pyramidal cells in the human neocortex that are preserved in Alzheimer's disease. *Neuropathol Appl Neurobiol* 29:316–320
- Rakic P (1995) A small step for the cell, a giant leap for mankind: a hypothesis of neocortical expansion during evolution. *Trends Neurosci* 18(9):383–388
- Rossion B, Dricot L, Devolder A, Bodart J-M, Crommelinck M, de Gelder B, Zootjes R (2000) Hemispheric asymmetries for whole-based and part-based face processing in the human fusiform gyrus. *J Cogn Neurosci* 12(5):793–802
- Schenker NM, Hopkins WD, Spocter MA, Garrison AR, Stimpson CD, Erwin JM, Hof PR, Sherwood CC (2010) Broca's area homologue in chimpanzees (*Pan troglodytes*): probabilistic mapping, asymmetry, and comparison to humans. *Cereb Cortex* 20(3):730–742
- Seldon HL (1981a) Structure of human auditory cortex: I. Cytoarchitectonics and dendritic distributions. *Brain Res* 229:277–294
- Seldon HL (1981b) Structure of human auditory cortex: II. Axon distributions and morphological correlates of speech perception. *Brain Res* 229:295–310
- Sherwood CC, Stimpson CD, Raghanti MA, Wildman DE, Uddin M, Grossman LI, Goodman M, Redmond JC, Bonar CJ, Erwin JM, Hof PR (2006) Evolution of increased glia-neuron ratios in the human frontal cortex. *Proc Natl Acad Sci USA* 103:13606–13611
- Sherwood CC, Wahl E, Erwin JM, Hof PR, Hopkins WD (2007) Histological asymmetries of primary motor cortex predict handedness in chimpanzees (*Pan troglodytes*). *J Comp Neurol* 503:525–537
- Skoglund TS, Pascher R, Berthold CH (2004) Aspects of the organization of neurons and dendritic bundles in primary somatosensory cortex of the rat. *Neurosci Res* 50:189–198
- Spocter MA, Hopkins WD, Garrison AR, Bauernfeind AL, Stimpson CD, Hof PR, Sherwood CC (2010) Wernicke's area homologue in chimpanzees (*Pan troglodytes*) and its relation to the appearance of modern human language. *Proc Biol Sci* 277(1691):2165–2174
- Taubert J, Parr LA (2010) Geometric distortions affect face recognition in chimpanzees (*Pan troglodytes*) and monkeys (*Macaca mulatta*). *Anim Cogn* 14:35–43
- Teunisse JP, de Gelder B (2001) Impaired categorical perception of facial expressions in high-functioning adolescents with autism. *Child Neuropsychol* 7(1):1–14
- Tsao DY, Moeller S, Freiwald WA (2008) Comparing face patch systems in macaques and humans. *Proc Natl Acad Sci USA* 105(49):19514–19519
- Van Kooten IA, Palmen SJ, von Cappeln P, Steinbusch HW, Korr H, Heinsen H, Hof PR, van Engeland H, Schmitz C (2008) Neurons in the fusiform gyrus are fewer and smaller in autism. *Brain* 131:987–999
- Von Economo C, Koskinas GN (1925) *Die Cytoarchitektonik der Hirnrinde des Erwachsenen Menschen*. Springer, Berlin (Germany) (Translated by Dr Lee Seldon)
- Wilson HR, Diaconescu A (2006) Learning alters local face space geometry. *Vision Res* 46:4143–4151
- Young MP, Yamane S (1992) Sparse population coding of faces in the inferotemporal cortex. *Science* 256:1327–1331
- Zatorre RJ, Belin P (2001) Spectral and temporal processing in human auditory cortex. *Cereb Cortex* 11:946–953
- Zhu Q, Song Y, Hu S, Li X, Tian M, Zhen Z, Dong Q, Kanwisher N, Liu J (2010) Heritability of the specific cognitive ability of face perception. *Curr Biol* 20(2):137–142